Elucidating the Photoluminescence Quenching in Ensulizole: An Artificial Water Soluble Sunscreen

Muhammad Mubeen
Quaid-i-Azam University
Muhammad Adnan Khalid
Quaid-i-Azam University
Maria Mukhtar
Quaid-i-Azam University
Saba Shahrum
Quaid-i-Azam University
Shanila Zahra
Quaid-i-Azam University
Saima Shabbir
Institute of Space Technology
Azhar Iqbal (aiqbal@qau.edu.pk)
Quaid-i-Azam University https://orcid.org/0000-0002-2616-3778

Research Article

Keywords: Sunscreen, Ensulizole, Photoluminescence, Time resolved, Quenching

Posted Date: March 19th, 2021

DOI: https://doi.org/10.21203/rs.3.rs-287999/v1

Abstract

Employing natural or artificial sunscreens is essential to protect the skin from ultraviolet radiations that cause premature aging and develop melanoma and other forms of skin cancer. The 2-Phenylbenzimidazole-5-sulfonic acid, commonly known as ensulizole is a water-soluble artificial sunscreen that absorbs mostly UV-B (280 nm − 315 nm) radiations and protects the skin against the harmful effects of these radiations. Steady-state absorption indicates a strong absorption feature at 303 nm and a weak at 316 nm that have been identified as $\pi \rightarrow \pi^*$ and $n \rightarrow \pi^*$ transitions, respectively. The photoluminescence (PL) spectra indicate that the PL of ensulizole is less Stokes-shifted in polar solvents and more Stokes-shifted in non-polar solvents. The average PL lifetime of ensulizole is longer in non-polar solvents as compared to polar solvents and it exhibits the shortest PL lifetime in aqueous medium that signifies its efficiency in water. This suggests in non-polar solvents intersystem crossing is the dominant mode of relaxation of the excited $\pi\pi^*$ state. Furthermore, an increase of pH of ensulizole solution decreases the PL intensity and the lifetime. Stern-Volmer equation is employed to evaluate bimolecular quenching rate constant k_q that suggests the diffusional dynamic mode of PL quenching is operative.

1. Introduction

The sunscreens act as protective coating for DNA mutation against UV radiations [1–4]. The extreme sun exposure could cause skin erythema [5] and tanning, which had been known since centuries, however the real mechanism was hitherto unclear [6]. Protection against sunlight supports to avert skin damage from unnecessary and extended contact to the sunlight. Excessive exposure to the sunlight can perform a major role in degenerative variations in the skin like photoaging and skin cancer [7–12]. It has been proved that ultraviolet (UV) radiations cause erythema solare [13]. This necessitates use of chemical sunscreens for the protection of skin [14–16]. First ever-efficacious commercial sunscreen, “Ambre Solaire” [17] was comprised of UV radiations filter benzylsalicylate. In addition to this, many other effective compounds have been explored as sunscreens, which lead to a general adoption of 4-aminobenzoic acid and later benzophenones as sunscreen agents [18]. Now a days, a number of different UV absorbing molecules find their use in commercial sunscreens [19–21]. There are 27 registered compounds, which are used as UV-filter in Europe as sunscreens [8].

Some of the sunscreen components might have a hostile effects on human skin and it is referred as “sunscreen controversy” [19, 22–24], therefore it is necessary to investigate the exact way of action of a sunscreen in order to eliminate its detrimental effects. Sunscreens are formulated to absorb the UV-A (320–400 nm) and UV-B (280–320 nm) [6, 25, 26] components of sunlight that consequently plummet the possibility of skin cancers such as melanoma or squamous cell carcinoma [27, 28]. Sunscreens in general consist of a substantial carrier oil, photostable inorganic particulates (ZnO and/or TiO_2) tend to absorb, reflect and scatter some part of the incident radiation) along with organic molecules having extended conjugation. These conjugated organic molecules provide photo-protection, without any photodegradation and phototoxicity. Numerous organic molecules used in sunscreens contain aromatic rings conjugated to carbonyl groups like oxybenzone, avobenzone, cinnamates (e.g. ferulic acid and caffeic acid), and salicilates [29–31]. Such molecules provide photo-protection by means of their high ultraviolet absorption

cross-sections and high internal conversion efficiencies. The absorption of UV radiations leads to electronic excitation and absorbed energy is quickly diffused through intramolecular vibrational energy redistribution (IVR) and dissipates it in the form of heat within the sunscreen [31–33].

2-Phenylbenzimidazole-5-sulfonic acid commonly known as “ensulizole” [34] is an effective and recommended sunscreen agent [7, 35–37] and it is a part of many commercially available sunscreen products [38]. Therefore, it is essential to study the photophysical properties of this compound in order to have a thorough understanding of its mode of action against absorbed UV radiations. To the best of our knowledge, first time the PL dynamics have been studied following excitation at 306 nm. The steady-state photoluminescence (SSPL) and time-resolved photoluminescence (TRPL) techniques are employed to investigate the PL dynamics of ensulizole both in solid-phase and as well as in solution form in different solvents, for instance, in CCl_4, acetone, water, methanol and ethanol. The PL kinetics demonstrates the average PL lifetime is longer in non-polar solvents than polar solvents. It has also been observed that with an increase in hydrogen ion (H^+) concentration, PL quenches and the average PL lifetime decreases due to the reduction in delocalization of π-electrons of ensulizole. This leads to the evaluation of bimolecular fluorescence quenching rate constant k_q, which has been estimated ≅ 2.945×10^7 M^{-1} s^{-1}. This work particularly addresses the effects of solvents polarity and the pH on the fluorescence dynamics of ensulizole that have not been explored thoroughly yet. These findings would prove a step forward towards understanding the mechanism of absorbed UV energy dissipation pathways in this important water-soluble sunscreen component.

2. Experiment And Methods

2.1. Materials

Ensulizole (98%) was purchased from Tokyo Chemical Industry (TCI) and was used without any further treatment. Deionized water was used for all aqueous-phase measurements. Acetone (Merck, 99.5%), methanol (AR, 99.9%) and ethanol (AR, 99.9%) were purchased from RCI Labscan and tetrachloromethane (99.8%) was purchased from Riedel-de Haen and was used as received without any further purification treatment.

2.2. Characterization Methods

The liquid samples of ensulizole were prepared in deionized water, tetrachloromethane, ethanol, methanol and acetone for UV-Vis absorption, SSPL and TRPL measurements at room temperature. The concentration of all liquid samples solutions was 1μM. Shimadzu UV-1601 spectrophotometer was used to measure the UV–Vis absorption spectrum at room temperature. All the samples were examined using the quartz cuvettes. The SSPL and TRPL analysis were conducted by Pico Quant Fluo Time 300 (FT-300) spectrophotometer as described in our previous work [39–41]. Briefly, the SSPL spectrum was measured following excitation at 306 nm with a pulsed LED excitation (PLS-300) source. The pulse duration of PLS-300 is ≅416 ps and its pulse energy is≅0.077 pJ. In order to filter the residual light of excitation source and to avoid second order

the long-pass color filter FGL400 was used. The aqueous paste of ensulizole was applied on quartz slide in the form of a thin film and was used for SSPL and TRPL measurements in solid form.

3. Results And Discussion

The UV-Vis absorption spectra of ensulizole in different solvents such as carbon tetrachloride, acetone, water, methanol and ethanol is displayed in Fig. 1(a). In polar neutral medium, ensulizole exists in monoanionic form and its sulfonic acid group donates proton that is accepted by the polar solvents like water, methanol and ethanol and subsequently stabilize the conjugate base of ensulizole. Removal of one or both protons from ensulizole results in an increase of delocalization of electrons, which tends to cause a red-shift in the UV absorption spectrum. The imidazole ring proton does not detach due to the neutral medium. For the removal of the imidazole ring proton, highly basic medium (pH =12 or above) is required. This is evidenced by Fig. 1(b), where a slight red-shift in the UV spectrum is observed in case of methanol and ethanol as compared to water. This is attributed to the electron releasing inductive effect [42] of methyl (CH_3-) moiety in methanol and ethyl (C_2H_5-) moiety in ethanol, which stabilizes both the protonated methanol and protonated ethanol.

As the ethyl- group has greater electron donating inductive effect, therefore, the absorption peak of ensulizole in ethanol is more red-shifted than in methanol, which in turn is more red-shifted than water, as it does not offer any such inductive stabilization effect. Acetone is a weakly polar solvent. It does not facilitate the ionization process as polar solvents demonstrate, for instance water, methanol and ethanol. This is manifested by the less solubility of ensulizole in acetone. Therefore, ensulizole shows a blue-shift in UV absorption spectra as compare to water, Fig. 1(a). The ensulizole is more soluble in carbon tetrachloride (CCl_4) due to non-polar interactions and these interactions do not favour the ionization of sulfonic acid group proton of ensulizole. Therefore, ensulizole remains undissociated in CCl_4 and its UV-Vis absorption spectrum exhibits a blue-shift as displayed by Fig. 1(a). The reaction scheme 1 displays the proposed mechanism of proton transfer in various solvents.

Some of the polar solvent molecules are converted into their respective conjugate acids form and remaining free solvent molecules develop hydrogen bonding with ensulizole at specific sites. The hydrogen bonding interaction affects the electronic excitations, in general an increase in solvent polarity causes a blue-shift in $n\rightarrow\pi^*$ transitions and a red-shift in $\pi\rightarrow\pi^*$ transitions [8].

The UV-Vis absorption spectra of ensulizole in water at pH $\leq$ 2 (Fig. 1(b)) demonstrate in strongly acidic conditions the ensulizole exists as undissociated acid. It exhibits an absorption peak at ~300 nm because of $\pi\rightarrow\pi^*$ transition and a shoulder at 314 nm due to $n\rightarrow\pi^*$ transition. As ensulizole is a weak acid (pKa_1 = 4 and pKa_2 = 11.9), so its solution is mildly acidic (pH = 6) when dissolved in water. It is the sulfonic acid group proton, which dissociates under these conditions and the absorption spectrum at this pH is slightly red-shifted. Reaction scheme 2 presents the proposed mechanism of proton transfer in different pH environments.

In highly alkaline medium (i.e., at pH >12), both the sulfonic acid and imine moieties protons of ensulizole are removed and the absorption peak even further red-shifts at this pH. The red-shift occurs due to increase in the delocalization of the π-electrons. The pronounced red-shift observation following removal of imine proton confirms the N-H group in imidazole ring is the chromophore and controls the photochemistry of ensulizole following excitation at 306 nm, as substantiated by laser flash photolysis experiments [43].

Since it has been justified above with the help of UV-Vis measurements that ππ* state along the N-H coordinate of imidazole ring will be excited at 306 nm with pulsed PLS excitation source. Henceforth, all the results of SSPL and TRPL measurements will be discussed after pulsed excitation at 306 nm. The SSPL spectra of ensulizole in solid form as well as in solution form in different solvents is displayed by Fig. 2(a). Following excitation at 306 nm the PL spectrum of ensulizole exhibits a peak at ≅445 nm in solid form as well as in slightly polar or non-polar solvents, like acetone and CCl_4, where there is no or very weak solute-solvent interactions exist. In polar solvents like methanol, ethanol and water the PL spectra of ensulizole exhibits a pronounced blue-shift and the PL peaks maxima moves to 412 nm as compare to slightly polar or non-polar solvents ($\lambda_{emission}$ = 445 nm) like acetone and CCl_4, Fig.2 (a). This trend can be attributed to the occurrence of hydrogen bonding between the aforementioned polar solvents and the ensulizole solute molecules.

Polar solvents like water, methanol and ethanol develop hydrogen bonding with ensulizole and due to this effect, non-bonding electrons on the nitrogen and oxygen atoms are engaged with the solvent molecules. This results in decrease of the delocalization of non-bonding electrons and consequently a blue-shift in PL spectrum is observed. Slightly polar or non-polar solvents like acetone and CCl_4 are unable to develop hydrogen bonding with the hetero-atoms of ensulizole, so the lone pairs of electrons are unrestricted and enhance the delocalization of π-electrons and causes a red-shift in the PL spectrum. A major evidence in this regard is the SSPL spectrum of ensulizole in the solid-state sample where there no solute-solvent interactions are possible. Amongst the polar solvents, SSPL spectra exhibit a slight red-shifted tail, which is more pronounced in water as compared to the ethanol and methanol. This is probably due to the polarity of the solvent and the delocalization effect, as justified above. The SSPL spectra of ensulizole in non-polar solvents are much broader as compared to the polar solvents. This is attributed to the enhanced delocalization effect in non-polar solvents. A slight red-shift in the SSPL spectra of ensulizole is observed in the acidic medium Fig. 2 (b). This again can be attributed to the fact that the increase in pH results in enhancement of delocalization and these observations are in consistent with the UV-Vis absorption measurements.

In order to assess the lifetime of ππ* state the PL kinetics is also measured. The ensulizole samples were excited at 306 nm and the PL decay kinetics was monitored at room temperature. Fig. 3 (a) depicts the PL decay kinetics of ensulizole in different solvents. The PLS-306 LED excitation source along with the electronics of time-correlated single photon-counting (TCSPC) setup allow conducting the measurements with a time-resolution of 500 ps. It is a well-known fact that an increase of solute-solvent interaction facilitates the internal conversion process. This leads to a decrease in fluorescence efficiency [44]. Reduction in the fluorescence efficiency is directly related to shortening of fluorescence lifetime. In aforementioned polar solvents, the ensulizole exhibits short PL lifetime and the PL decay kinetics is found to be

monoexponential **(Fig.3 (a))**, in comparison to the non-polar solvents due to solute-solvent interactions, which are present in former and are absent in the latter. Thus, the polar solvents due to existence of solute-solvent interaction increase the internal conversion (IC) rate and decrease the fluorescence lifetime, confirming the ensulizole can be the most effective sunscreen in polar solvents particularly in water, where the ππ* state exhibits the shortest lifetime. To further corroborate this finding, the solvent polarity was gradually decreased that resulted in enhancement of PL lifetime. In order to eliminate the solvent-solute interactions the measurements were also conducted in the solid film of the ensulizole **(Fig. 3(b))**. The measured PL kinetics of all the solution-phase samples is fitted by a suitable exponential decay model (eq. 1) and the fitting parameters are displayed in **table 1**. The solid sample of ensulizole exhibited the longest PL lifetime (τ_{av} = 6.879 ns) and this can be attributed to the population transfer from the single to triplet state by intersystem crossing (ISC) process. The average PL lifetimes were estimated by eq. (2) using the time constants and the coefficients extracted from eq. (1). The τ_{av} and the extracted fitting parameters from the aforementioned equations (1) & (2) are presented in table 1.

$$Y = Y_0 + \sum_{i=1}^{n} A_i e^{\frac{-(x-x_0)}{\tau_i}} \qquad (1)$$

$$\tau_{average} = \sum_{i=1}^{n} \frac{A_i \tau_i}{A_i} \qquad (2)$$

Here A_i, x_0 and t_i are the associated coefficients, time zero and the time constants, respectively.

Table 1: The fitting parameters extracted from a unimolecular (monoexponential), biexponential, triexponential and tetraexponentail decay models for ensulizole in different solvents.

Sample ID.	A_1	τ_1 (ns)	A_2	τ_2 (ns)	A_3	τ_3 (ns)	A_4	τ_4 (ns)	$\tau_{(Average)}$ (ns)
Ensulizole film	1849.5	7.229	10958	1.757	1302.5	34.042	131.20	143.40	6.879
CCl_4	1808.1	9.957	10915	1.869	874.6	43.363	—	—	5.918
Acetone	2124.1	28.762	15951	1.567	—	—	—	—	4.763
Ethanol	15557.6	2.847	—	—	—	—	—	—	2.847
Methanol	16167.9	2.505	—	—	—	—	—	—	2.505
Water	16382	1.688	—	—	—	—	—	—	1.688

In order to study the effect of pH on the excited ππ* state lifetime, the PL kinetics was also conducted in various pH environments in water as solvent, **Fig. 3(c)**. It displays different PL decay kinetics for ensulizole in mono-anionic form i.e., at pH = 6, in molecular form i.e., at pH= 2 and in highly basic medium i.e., at pH = 14. The measured PL kinetics is best fitted by biexponential decay model for pH 2 – 6 and a unimolecular

(monoexponential) decay model for pH 8 - 14, **table 2**. The increase in PL lifetime by increasing the pH from acidic to highly basic medium is due to enhanced stabilization of π-electronic system after removal of the second proton from the imino group. These findings again confirm that imidazole ring is the chromophore of the ensulizole and are in consistent with the steady-state absorption analysis. This inference is also in accordance with previously reported laser flash photolysis experiments, where following excitation at 266 nm the dissociation of imino group and the formation of dianion of ensulizole through double deprotonation has been observed [43]. Altough these experiments do not exactly mimic the TRPL measuremnets performed here, but as justified above the high pH extracts the second H^+ from the imino group that further stablizes the π-electron system and enhnaces the PL lifetime.

Table 2: The fitting parameters extracted from a unimolecular (monexponential), biexponentail decay kinetics models for ensulizole at different pH.

Sr. no.	pH	A_1	τ_1 (ns)	A_2	τ_2 (ns)	$\tau_{(Average)}$ (ns)	τ_o/τ
1.	2	17283	1.367	187.5	3.481	1.389	1.709
2.	4	15857	1.485	27.51	16.38	1.511	1.572
3.	6	16262	1.678	17.42	14.84	1.692	1.404
4.	8	15009.5	1.910	—	—	1.911	1.243
5.	10	15551	2.056	—	—	2.056	1.156
6.	12	15522.4	2.347	—	—	2.347	1.012
7.	14	15190	2.376	—	—	2.375	1

The removal of the second H^+ and enhancement of the PL lifetime confirms that the photoexcited $\pi\pi^*$ state along the N-H coordinate of imidazole ring controls the photochemistry of ensulizole following excitation at 306 nm.

A gradual drop in PL intensity of ensulizole is observed with a decrease in pH value from 14 to 2 as shown in **Fig. 2 (b)**. This reflects a quenching role of hydrogen ions (H^+) in this process. With increase in H^+ concentration (decrease in pH value), a decrease in PL intensity and average PL lifetime has been observed. By applying Stern-Volmer equation [45,46] (eqs. 3 & 4) to the measured PL data, a straight line with intercept equal to one is obtained **(Fig.3 (d))**, thus confirming the dynamic and diffusion controlled PL quenching of the ensulizole. The linear fit to the data enabled to evaluate the Stern-Volmer quenching constant $K_{SV,}$ 0.06995 M^{-1}, where $K_{SV} = k_q \times \tau_o$.

$$\frac{\tau_0}{\tau} = 1 + K_{sv}[Q] \quad (3)$$

$$\frac{\tau_0}{\tau} = 1 + K_q \tau_0 [H^+] \quad (4)$$

Where [Q] is concentration of quencher, τ_o is average lifetime in the absence of quencher, τ is average lifetime in the presence of quencher and K_q is bimolecular quenching rate constant (eq. 4). The estimated value of bimolecular quenching constant is 2.945×10^7 M^{-1} s^{-1}. In this study, we quantitatively demonstrate the lifetime of ππ* state locating on N-H coordinate of imidazole ring of ensulizole that strongly depends on the solvent polarity and the pH of the medium. Our future studies will focus on the photochemistry of ensulizole attached semiconductor quantum dots (QDs) to address how the QDs alter the photochemistry of the chromophore, in particular the N-H coordinate.

4. Conclusions

The TRPL measurements confirmed the ensulizole could be most effective sunscreen in water because it exhibited shortest PL lifetime. It further demonstrated the average PL lifetime of $\pi\pi^*$ ensulizole was higher in non-polar solvents than in polar solvents particularly in H_2O. This was attributed to solute-solvent interactions, which were present in polar solvents and absent in non-polar solvents. The polar solvents encouraged the IC and reduced the lifetime of the excited ππ* state. A solid evidence in this regard was the much longer PL lifetime (τ_{av} = 6.879 ns) of ensulizole in the solid phase. The measured PL kinetics also suggested that in non-polar solvents and in solid phase the probability of ISC increased by populating the triplet state thus resulting in the enhancement of the PL lifetime. It was observed that with decrease in pH value from 14 − 2, the PL intensity and hence average PL life time of ensulizole both reduced. This confirmed the H^+ behaved as fluorescence quencher and by applying Stern-Volmer equation, the dynamical quenching rate constant, K_q = 2.945×10^7 M^{-1} s^{-1} was estimated. These findings suggest the fluorescence and hence the photochemistry of ensulizole after excitation at 306 nm is greatly influenced by the pH and the solvent polarity and the repercussions of which will help to improve the understanding of underlying photochemistry of water soluble ensulizole and to increase its action in harsh environments.

Declarations

Acknowledgements

This work was performed within the Department of Chemistry Quaid-i-Azam University Islamabad. The authors gratefully acknowledge financial support by Higher Education Commission (HEC) Pakistan through research/equipment grants 20-3071/NRPU/R&D/HEC/13 and 6976/Federal/NRPU/R&D/HEC/2017.

Funding: The was supported by Higher Education Commission (HEC) Pakistan through research/equipment grants 20-3071/NRPU/R&D/HEC/13 and 6976/Federal/NRPU/R&D/HEC/2017.

Author Contributions: All authors contribute to the study of conception and design. Muhammad Mubeen performed the experiments and wrote the initial draft of the manuscript. Muhammad Adnan Khalid, Maria Mukhtar, Saba Shahrum and Sanila Zahra helped to conduct the experiments and data acquisition. Saima Shabbir commented on the manuscript and revised. Azhar Iqbal perceived the idea, acquired the funding, and supervised the work and writing of the manuscript.

Data Availability: All data generated or analyzed during this study are included.

Code Availability: All data were obtained using word, origin and Chemdraw.

Conflicts of interests/Competing Interests: There are no conflicts of interest to declare.

Ethics Approval: Not applicable

Consent to Participate: Not applicable

Consent of Publication: Not applicable

References

1. Bais AF, Lucas RM, Bornman JF, Williamson CE, Sulzberger B, Austin AT, Wilson SR, Andrady AL, Bernhard G, McKenzie RL (2018) Environmental effects of ozone depletion, UV radiation and interactions with climate change: UNEP Environmental Effects Assessment Panel, update 2017. Photochem Photobiol Sci 17:127-179
2. Bernhard GH, Neale RE, Barnes PW, Neale P, Zepp RG, Wilson SR, Andrady AL, Bais AF, McKenzie R, Aucamp P (2020) Environmental effects of stratospheric ozone depletion, UV radiation and interactions with climate change: UNEP Environmental Effects Assessment Panel, update 2019. Photochem Photobiol Sci 19:542-584
3. Kao M-H, Venkatraman RK, Sneha M, Wilton M, Orr-Ewing AJ (2021) Influence of the Solvent Environment on the Ultrafast Relaxation Pathways of a Sunscreen Molecule Diethylamino Hydroxybenzoyl Hexyl Benzoate. J Phys Chem A 125:636–645
4. Bacardit A, Cartoixà X (2020) Revisiting the Role of Irradiance in the Determination of Sunscreens' Sun Protection Factor. J Phys Chem Lett 11:1209-1214
5. Serrano Jareño MA, Moreno J (2013) Erythemal ultraviolet solar radiation doses received by young skiers. Photochem Photobiol Sci 12:1976-1983
6. Baker LA, Clark SL, Habershon S, Stavros VG (2017) Ultrafast Transient Absorption Spectroscopy of the Sunscreen Constituent Ethylhexyl Triazone. J Phys Chem Lett 8:2113-2118
7. Inbaraj JJ, Bilski P, Chignell CF (2002) Photophysical and Photochemical Studies of 2-Phenylbenzimidazole and UVB Sunscreen 2-Phenylbenzimidazole-5-sulfonic Acid. Photochem Photobiol 75:107-116
8. Herzog B, Amorós-Galicia L, Sohn M, Hofer M, Quass K, Giesinger J (2019) Analysis of photokinetics of 2'-ethylhexyl-4-methoxycinnamate in sunscreens. Photochem Photobiol Sci 18:1773-1781

9. Dondi D, Albini A, Serpone N (2006) Interactions between different solar UVB/UVA filters contained in commercial suncreams and consequent loss of UV protection. Photochem Photobiol Sci 5:835-843
10. Lewicka ZA, William WY, Oliva BL, Contreras EQ, Colvin VL (2013) Photochemical behavior of nanoscale TiO2 and ZnO sunscreen ingredients. J Photochem Photobiol A 263:24-33
11. Wright CY, du Preez DJ, Martincigh BS, Allen MW, Millar DA, Wernecke B, Blesic S (2020) A Comparison of Solar Ultraviolet Radiation Exposure in Urban Canyons in Venice, Italy and Johannesburg, South Africa. Photochem Photobiol 96:1148-1153
12. Sansomchai P, Jumpatong K, Lapinee C, Utchariyajit K (2021) Melientha suavis Pierre. Extract: antioxidant and sunscreen properties for future cosmetic development. CMUJ Nat Sci 20:e2021008
13. Löfgren S (2017) Solar ultraviolet radiation cataract. Experimental eye research 156:112-116
14. Urbach F (2001) The historical aspects of sunscreens. J Photochem Photobiol B 64:99-104
15. Hockberger PE (2002) A History of Ultraviolet Photobiology for Humans, Animals and Microorganisms. Photochem Photobiol 76:561-579
16. Lorenzen M, Racicot V, Strack D, Chapple C (1996) Sinapic acid ester metabolism in wild type and a sinapoylglucose-accumulating mutant of Arabidopsis. Plant Physiol 112:1625-1630
17. Ghazi S, Couteau C, Coiffard L (2010) What level of protection can be obtained using sun protective clothing? Determining effectiveness using an in vitro method. Int J Pharm 397:144-146
18. Lowe N (2006) An overview of ultraviolet radiation, sunscreens, and photo-induced dermatoses. Dermatol Clin 24:9-17
19. Lodén M, Beitner H, Gonzalez H, Edström D, Åkerström U, Austad J, Buraczewska-Norin I, Matsson M, Wulf H (2011) Sunscreen use: controversies, challenges and regulatory aspects. Br J Dermatol 165:255-262
20. Jansen R, Osterwalder U, Wang SQ, Burnett M, Lim HW (2013) Photoprotection: part II. Sunscreen: development, efficacy, and controversies. J Am Acad Dermatol 69:867.e1-867.e14
21. Mancebo SE, Hu JY, Wang SQ (2014) Sunscreens: a review of health benefits, regulations, and controversies. Dermatol Clin 32:427-438
22. Jansen R, Wang SQ, Burnett M, Osterwalder U, Lim HW (2013) Photoprotection: part I. Photoprotection by naturally occurring, physical, and systemic agents. J Am Acad Dermatol 69:853.e1-853.e12
23. Holmes AM, Kempson IM, Turnbull T, Paterson D, Roberts MS (2020) Penetration of zinc into human skin after topical application of nano zinc oxide used in commercial sunscreen formulations. ACS Appl Bio Mater 3:3640-3647
24. Erickson B (2020) More evidence sunscreens are absorbed through skin. Chem Eng News 98:16-16
25. Kasting JF, Siefert JL (2002) Life and the evolution of Earth's atmosphere. Science 296:1066-1068
26. Enchev V, Angelov I, Mantareva V, Markova N (2015) 2-Carbamido-1, 3-indandione–a Fluorescent Molecular Probe and Sunscreen Candidate. J Fluoresc 25 (6):1601-1614
27. Kanavy HE, Gerstenblith MR (2011) Ultraviolet radiation and melanoma. In J Cutan Med Surg 4:222-228
28. Burnett ME, Wang SQ (2011) Current sunscreen controversies: a critical review. Photodermatol Photoimmunol Photomed 27:58-67

29. Tan EM, Hilbers M, Buma WJ (2014) Excited-state dynamics of isolated and microsolvated cinnamate-based UV-B sunscreens. J Phys Chem Lett 5:2464-2468
30. Kockler J, Oelgemöller M, Robertson S, Glass BD (2012) Photostability of sunscreens. J Photochem Photobiol C 13:91-110
31. Karsili TN, Marchetti B, Ashfold MN, Domcke W (2014) Ab initio study of potential ultrafast internal conversion routes in oxybenzone, caffeic acid, and ferulic acid: Implications for sunscreens. J Phys Chem A 118:11999-12010
32. Baker LA, Horbury MD, Greenough SE, Coulter PM, Karsili TN, Roberts GM, Orr-Ewing AJ, Ashfold MN, Stavros VG (2015) Probing the ultrafast energy dissipation mechanism of the sunscreen oxybenzone after UVA irradiation. J Phys Chem Lett 6:1363-1368
33. Krishnan R, Nordlund TM (2008) Fluorescence dynamics of three UV-B sunscreens. J Fluoresc 18:203-217
34. Bastien N, Millau J-F, Rouabhia M, Davies RJH, Drouin R (2010) The sunscreen agent 2-phenylbenzimidazole-5-sulfonic acid photosensitizes the formation of oxidized guanines in cellulo after UV-A or UV-B exposure. J Invest Dermatol 130:2463-2471
35. Narla S, Lim HW (2020) Sunscreen: FDA regulation, and environmental and health impact. Photochem Photobiol 19:66-70
36. Gasparro FP (2000) Sunscreens, skin photobiology, and skin cancer: the need for UVA protection and evaluation of efficacy. Environ Health Perspect 108:71-78
37. Abdel-Ghany MF, Ayad MF, Mikawy NN (2018) Sensitive Synchronous Spectrofluorimetric Study of Certain Sunscreens Using Fluorescence Enhancers in Cosmeceutical Formulations. J Fluoresc 28:491-504
38. Diffey BL, Tanner PR, Matts PJ, Nash JF (2000) In vitro assessment of the broad-spectrum ultraviolet protection of sunscreen products. J Am Acad Dermatol 43:1024-1035
39. Saeed S, Channar PA, Larik FA, Saeed A, Nadeem MA, Iqbal A (2019) Charge/energy transfer dynamics in CuO quantum dots attached to photoresponsive azobenzene ligand. J Phys Chem A 371:44-49
40. Saeed S, Yin J, Khalid MA, Channar PA, Shabir G, Saeed A, Nadeem MA, Soci C, Iqbal A (2019) Photoresponsive azobenzene ligand as an efficient electron acceptor for luminous CdTe quantum dots. J Phys Chem A 375:48-53
41. Siddique Z, Payne JL, Irvine JT, Jagadamma LK, Akhter Z, Samuel ID, Iqbal A (2020) Effect of halide-mixing on tolerance factor and charge-carrier dynamics in (CH 3 NH 3 PbBr 3− x Cl x) perovskites powders. J Mater Sci 31:19415-19428
42. Teixeira RI, da Silva RB, Gaspar CS, de Lucas NC, Garden SJ (2021) Photophysical Properties of Fluorescent 2-(Phenylamino)-1, 10-phenanthroline Derivatives. Photochem Photobiol 97:47-60
43. Ji Y, Zhou L, Zhang Y, Ferronato C, Brigante M, Mailhot G, Yang X, Chovelon J-M (2013) Photochemical degradation of sunscreen agent 2-phenylbenzimidazole-5-sulfonic acid in different water matrices. Water Res 47:5865-5875

44. Senesi N (1990) Molecular and quantitative aspects of the chemistry of fulvic acid and its interactions with metal ions and organic chemicals: Part I. The electron spin resonance approach. Anal Chim Acta 232:51-75
45. Bose D, Sarkar D, Chattopadhyay N (2010) Probing the binding interaction of a phenazinium dye with serum transport proteins: a combined fluorometric and circular dichroism study. Photochem Photobiol 86:538-544
46. Koppal V, Melavanki R, Kusanur R, Patil N (2021) Analysis of Fluorescence Quenching of Coumarin Derivative under Steady State and Transient State Methods. J Fluoresc https://doi.org/10.1007/s10895-020-02663-3

Figures

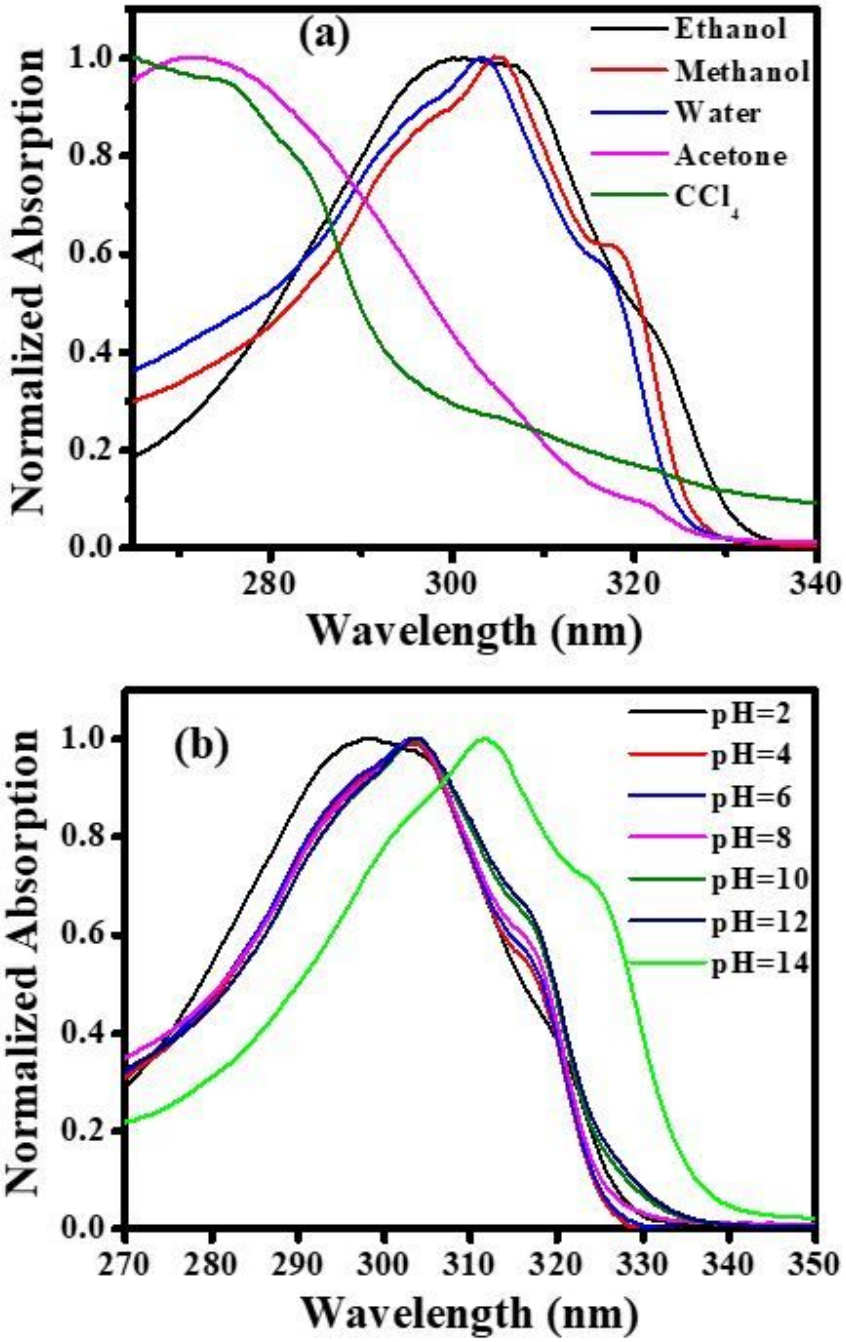

Figure 1

Comparison of steady-state UV-Vis absorption spectra of Ensulizole (a) in different solvents and (b) in water at different pH.

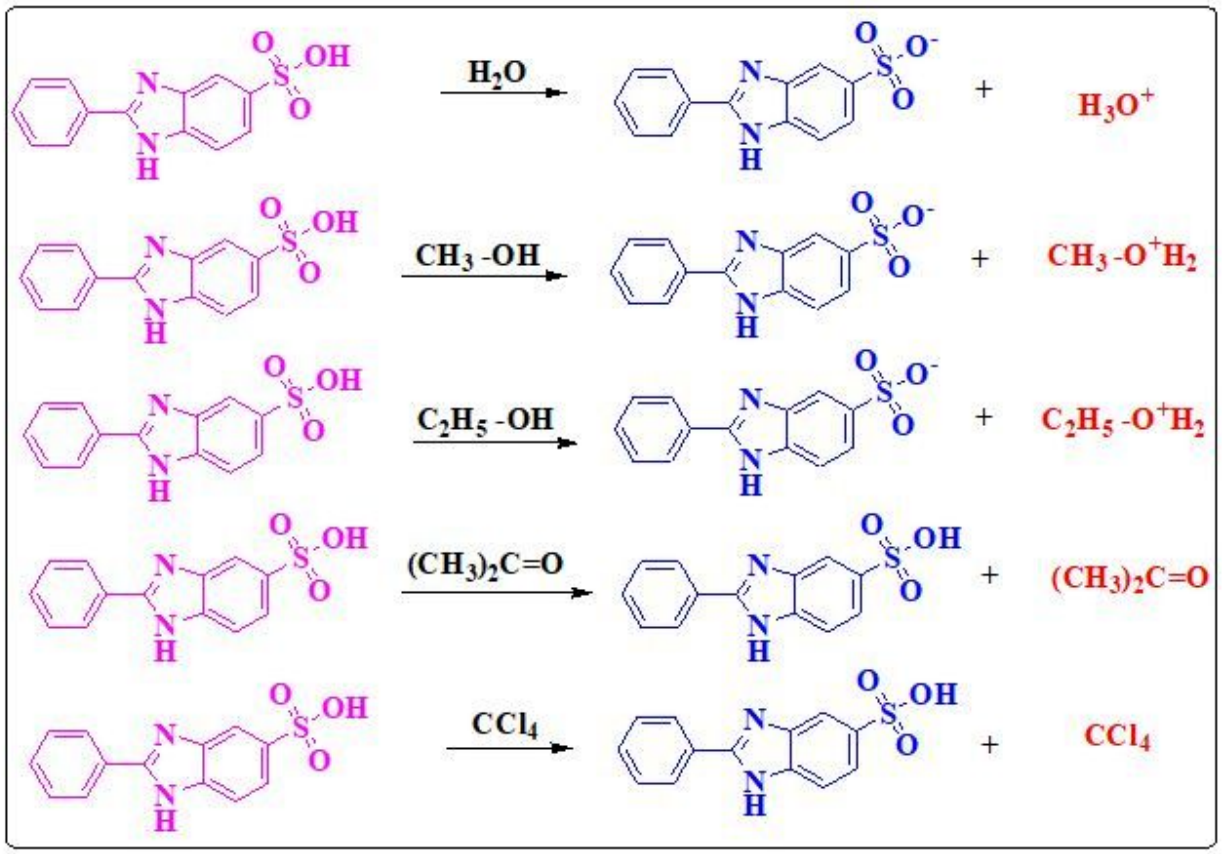

Figure 2

Proposed mechanism of proton transfer in different solvents.

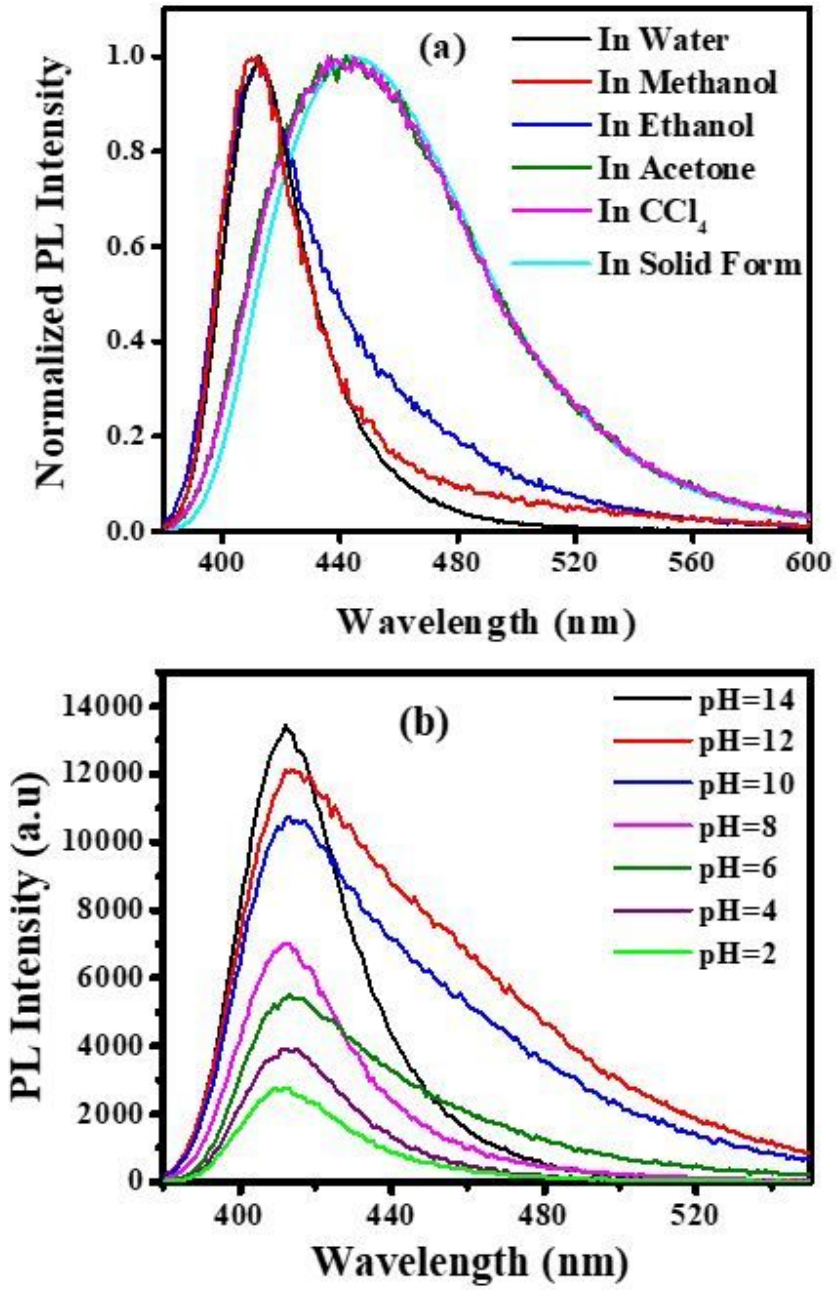

Figure 3

Effect of (a) various solvents interactions on the PL of ensulizole and (b) varying pH on the PL of ensulizole in water.

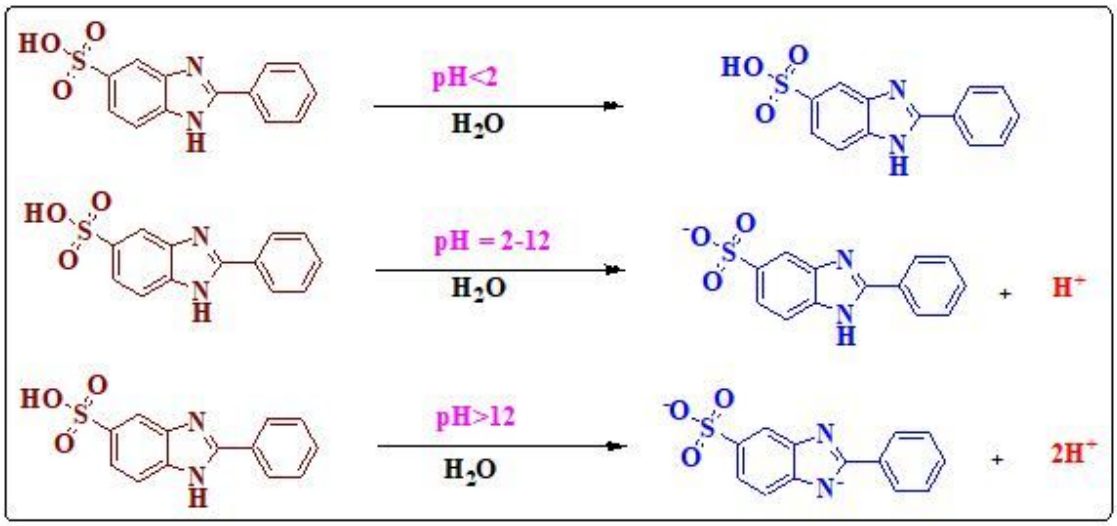

Figure 4

Proposed mechanism of proton transfer in ensulizole at different pH.

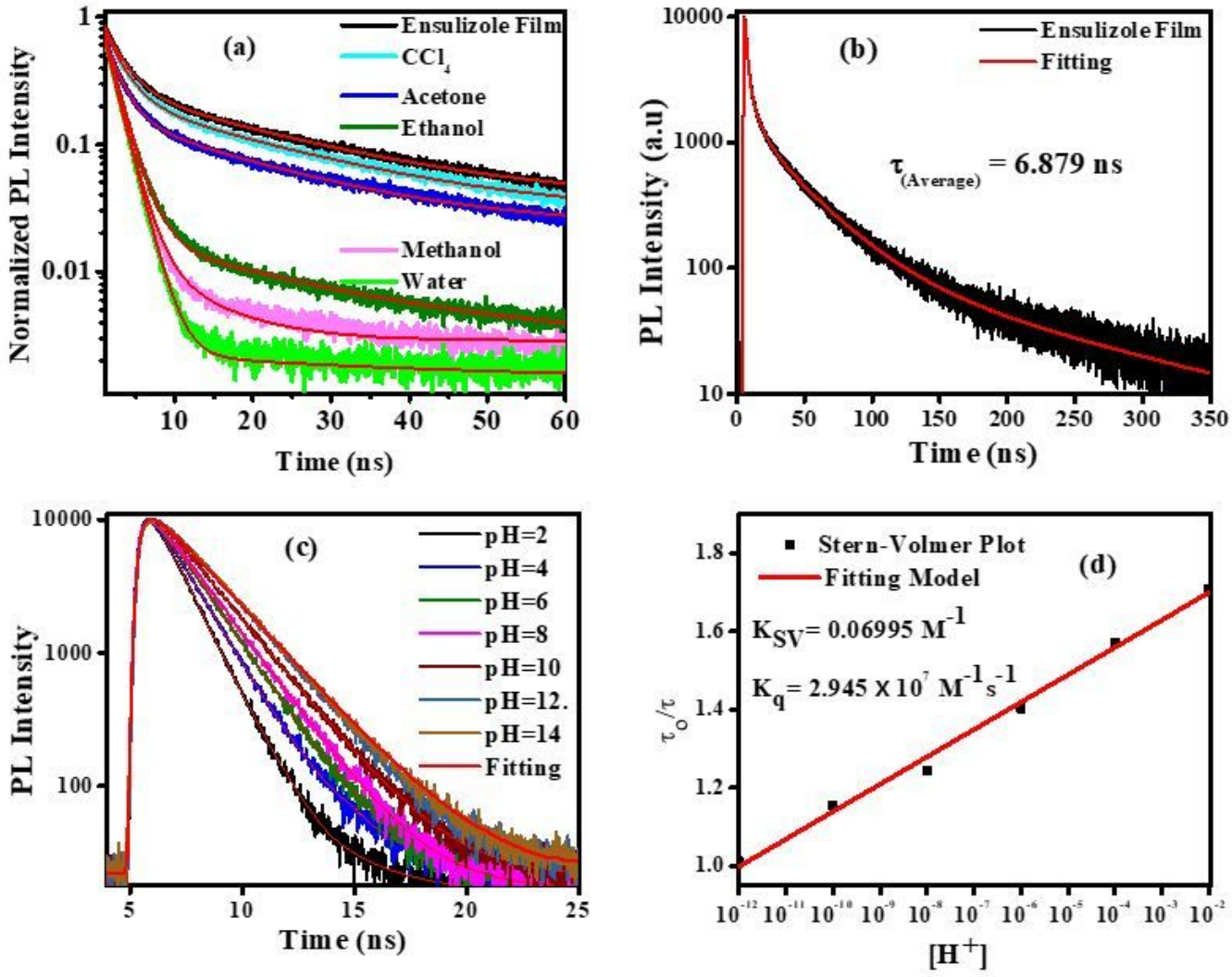

Figure 5

Comparison of (a) PL decay kinetics of ensulizole in various solvents and (b) PL decay kinetics over extended time delay of ensulizole solid film, after excitation at 306 nm. (c) PL decay kinetics of ensulizole in water at different pH. (d) Stern-Volmer plot. The solid red curves represent the best fits to the measured PL kinetics.

Supplementary Files

This is a list of supplementary files associated with this preprint. Click to download.

- TOC.jpg